Physics Letters B 277 (1992) 371–382
North-Holland

PHYSICS LETTERS B

# A measurement of $\sin^2\theta_w$ from the charge asymmetry of hadronic events at the $Z^0$ peak

DELPHI Collaboration

P. Abreu [a], W. Adam [b], F. Adami [c], T. Adye [d], T. Akesson [e], G.D. Alekseev [f], P. Allen [g], S. Almehed [e], S.J. Alvsvaag [h], U. Amaldi [i], E. Anassontzis [j], P. Antilogus [k], W.-D. Apel [l], R.J. Apsimon [d], B. Åsman [m], J.-E. Augustin [n], A. Augustinus [o], P. Baillon [i], P. Bambade [n], F. Barao [a], R. Barate [p], G. Barbiellini [q], D.Y. Bardin [f], A. Baroncelli [r], O. Barring [e], W. Bartl [b], M.J. Bates [s], M. Battaglia [t], M. Baubillier [u], K.-H. Becks [v], C.J. Beeston [s], M. Begalli [w], P. Beilliere [x], Yu. Belokopytov [y], P. Beltran [z], D. Benedic [aa], J.M. Benlloch [g], M. Berggren [n], D. Bertrand [ab], F. Bianchi [ac], M.S. Bilenky [f], P. Billoir [u], J. Bjarne [e], D. Bloch [aa], S. Blyth [s], V. Bocci [ad], P.N. Bogolubov [f], T. Bolognese [c], M. Bonapart [o], M. Bonesini [t], W. Bonivento [t], P.S.L. Booth [ae], P. Borgeaud [c], G. Borisov [y], H. Borner [i], C. Bosio [r], B. Bostjancic [i], O. Botner [af], B. Bouquet [n], C. Bourdarios [n], M. Bozzo [w], S. Braibant [ab], P. Branchini [r], K.D. Brand [ag], R.A. Brenner [ah], H. Briand [u], C. Bricman [ab], R.C.A. Brown [i], N. Brummer [o], J.-M. Brunet [x], L. Bugge [ai], T. Buran [ai], H. Burmeister [i], J.A.M.A. Buytaert [i], M. Caccia [i], M. Calvi [t], A.J. Camacho Rozas [aj], A. Campion [ae], T. Camporesi [i], V. Canale [ad], F. Cao [ab], F. Carena [i], L. Carroll [ae], C. Caso [w], E. Castelli [q], M.V. Castillo Gimenez [g], A. Cattai [i], F.R. Cavallo [ak], L. Cerrito [ad], A. Chan [al], P. Charpentier [i], L. Chaussard [n], J. Chauveau [u], P. Checchia [ag], G.A. Chelkov [f], L. Chevalier [c], P. Chliapnikov [y], V. Chorowicz [u], R. Cirio [ac], M.P. Clara [ac], P. Collins [s], J.L. Contreras [am], R. Contri [w], G. Cosme [n], F. Couchot [n], H.B. Crawley [al], D. Crennell [d], G. Crosetti [w], M. Crozon [x], J. Cuevas Maestro [aj], S. Czellar [ah], S. Dagoret [n], E. Dahl-Jensen [an], B. Dalmagne [n], M. Dam [ai], G. Damgaard [an], G. Darbo [w], E. Daubie [ab], P.D. Dauncey [s], M. Davenport [i], P. David [u], W. Da Silva [u], C. Defoix [x], D. Delikaris [i], S. Delorme [i], P. Delpierre [x], N. Demaria [ac], A. De Angelis [q], M. De Beer [c], H. De Boeck [ab], W. De Boer [l], C. De Clercq [ab], M.D.M. De Fez Laso [g], N. De Groot [o], C. De La Vaissiere [u], B. De Lotto [q], A. De Min [t], H. Dijkstra [i], L. Di Ciaccio [ad], F. Djama [aa], J. Dolbeau [x], M. Donszelmann [o], K. Doroba [ao], M. Dracos [i], J. Drees [v], M. Dris [ap], Y. Dufour [x], W. Dulinski [aa], L.-O. Eek [af], P.A.-M. Eerola [i], T. Ekelof [af], G. Ekspong [m], A. Elliot Peisert [ag], J.-P. Engel [aa], D. Fassouliotis [ap], M. Feindt [i], A. Fenyuk [y], M. Fernandez Alonso [aj], A. Ferrer [g], T.A. Filippas [ap], A. Firestone [al], H. Foeth [i], E. Fokitis [ap], P. Folegati [q], F. Fontanelli [w], K.A.J. Forbes [ae], B. Franek [d], P. Frenkiel [x], D.C. Fries [l], A.G. Frodesen [h], R. Fruhwirth [b], F. Fulda-Quenzer [n], K. Furnival [ae], H. Furstenau [l], J. Fuster [i], G. Galeazzi [ag], D. Gamba [ac], C. Garcia [g], J. Garcia [aj], C. Gaspar [i], U. Gasparini [ag], P. Gavillet [i], E.N. Gazis [ap], J.-P. Gerber [aa], P. Giacomelli [i], R. Gokieli [i], V.M. Golovatyuk [f], J.J. Gomez Y Cadenas [i], A. Goobar [m], G. Gopal [d], M. Gorski [ao], V. Gracco [w], A. Grant [i], F. Grard [ab], E. Graziani [r], G. Grosdidier [n], E. Gross [i], P. Grosse-Wiesmann [i], B. Grossetete [u], S. Gumenyuk [y], J. Guy [d], F. Hahn [i], M. Hahn [l], S. Haider [o], Z. Hajduk [aq], A. Hakansson [e], A. Hallgren [af], K. Hamacher [v], G. Hamel De Monchenault [c], F.J. Harris [s], B.W. Heck [i], T. Henkes [i], J.J. Hernandez [g], P. Herquet [ab], H. Herr [i], I. Hietanen [ah], C.O. Higgins [ae], E. Higon [g], H.J. Hilke [i], S.D. Hodgson [s], T. Hofmokl [ao], R. Holmes [al], S.-O. Holmgren [m], D. Holthuizen [o], P.F. Honore [x], J.E. Hooper [an], M. Houlden [ae], J. Hrubec [b], P.O. Hulth [m], K. Hultqvist [m], D. Husson [aa], P. Ioannou [j],

D. Isenhower [i], P.-S. Iversen [h], J.N. Jackson [ae], P. Jalocha [aq], G. Jarlskog [e], P. Jarry [c], B. Jean-Marie [n], E.K. Johansson [m], D. Johnson [ae], M. Jonker [i], L. Jonsson [e], P. Juillot [aa], G. Kalkanis [j], G. Kalmus [d], F. Kapusta [u], M. Karlsson [i], S. Katsanevas [j], E.C. Katsoufis [ap], R. Keranen [ah], J. Kesteman [ab], B.A. Khomenko [f], N.N. Khovanski [f], B. King [ae], N.J. Kjaer [i], H. Klein [i], W. Klempt [i], A. Klovning [h], P. Kluit [o], J.H. Koehne [ℓ], B. Koene [o], P. Kokkinias [z], M. Kopf [ℓ], M. Koratzinos [ac], K. Korcyl [aq], A.V. Korytov [f], V. Kostiukhin [y], M. Kostrikov [y], C. Kourkoumelis [j], P.H. Kramer [v], T. Kreuzberger [b], J. Krolikowski [ao], I. Kronkvist [e], J. Krstic [s], U. Kruener-Marquis [v], W. Krupinski [aq], W. Kucewicz [t], K. Kurvinen [ah], C. Lacasta [g], C. Lambropoulos [z], J.W. Lamsa [aℓ], L. Lanceri [q], V. Lapin [y], J.-P. Laugier [c], R. Lauhakangas [ah], G. Leder [b], F. Ledroit [p], R. Leitner [i], Y. Lemoigne [c], J. Lemonne [ab], G. Lenzen [v], V. Lepeltier [n], A. Letessier-Selvon [u], E. Lieb [v], D. Liko [b], E. Lillethun [h], J. Lindgren [ah], R. Lindner [v], A. Lipniacka [ao], I. Lippi [ag], R. Llosa [am], B. Loerstad [e], M. Lokajicek [f], J.G. Loken [s], A. Lopez-Fernandez [n], M.A. Lopez Aguera [aj], M. Los [o], D. Loukas [z], A. Lounis [aa], J.J. Lozano [g], P. Lutz [x], L. Lyons [s], G. Maehlum [i], J. Maillard [x], A. Maltezos [z], F. Mandl [b], J. Marco [aj], M. Margoni [ag], J.-C. Marin [i], A. Markou [z], T. Maron [v], S. Marti [g], L. Mathis [aℓ], F. Matorras [aj], C. Matteuzzi [t], G. Matthiae [ad], M. Mazzucato [ag], M. Mc Cubbin [ae], R. Mc Kay [aℓ], R. Mc Nulty [ae], E. Menichetti [ac], G. Meola [w], C. Meroni [t], W.T. Meyer [aℓ], M. Michelotto [ag], W.A. Mitaroff [b], G.V. Mitselmakher [f], U. Mjoernmark [e], T. Moa [m], R. Moeller [an], K. Moenig [i], M.R. Monge [w], P. Morettini [w], H. Mueller [ℓ], W.J. Murray [d], B. Muryn [n], G. Myatt [s], F. Naraghi [u], F.L. Navarria [ak], P. Negri [t], B.S. Nielsen [an], B. Nijjhar [ae], V. Nikolaenko [y], V. Obraztsov [y], K. Oesterberg [ah], A.G. Olshevski [f], R. Orava [ah], A. Ostankov [y], A. Ouraou [c], M. Paganoni [t], R. Pain [u], H. Palka [o], T. Papadopoulou [ap], L. Pape [i], A. Passeri [r], M. Pegoraro [ag], J. Pennanen [ah], V. Perevozchikov [y], M. Pernicka [b], A. Perrotta [ak], F. Pierre [c], M. Pimenta [a], O. Pingot [ab], M.E. Pol [i], G. Polok [aq], P. Poropat [q], P. Privitera [ℓ], A. Pullia [t], D. Radojicic [s], S. Ragazzi [t], P.N. Ratoff [ar], A.L. Read [ai], N.G. Redaelli [t], M. Regler [b], D. Reid [ae], P.B. Renton [s], L.K. Resvanis [j], F. Richard [n], M. Richardson [ae], J. Ridky [f], G. Rinaudo [ac], I. Roditi [i], A. Romero [ac], I. Roncagliolo [w], P. Ronchese [ag], C. Ronnqvist [ah], E.I. Rosenberg [aℓ], U. Rossi [ak], E. Rosso [i], P. Roudeau [n], T. Rovelli [ak], W. Ruckstuhl [o], V. Ruhlmann [c], A. Ruiz [aj], K. Rybicki [aq], H. Saarikko [ah], Y. Sacquin [c], G. Sajot [p], J. Salt [g], E. Sanchez [g], J. Sanchez [am], M. Sannino [w], M. Schaeffer [aa], S. Schael [ℓ], H. Schneider [ℓ], M.A.E. Schyns [v], F. Scuri [q], A.M. Segar [s], R. Sekulin [d], M. Sessa [q], G. Sette [w], R. Seufert [ℓ], R.C. Shellard [i], P. Siegrist [c], S. Simonetti [w], F. Simonetto [ag], A.N. Sissakian [f], T.B. Skaali [ai], G. Skjevling [ai], G. Smadja [c,k], N. Smirnov [y], G.R. Smith [d], R. Sosnowski [ao], T.S. Spassoff [p], E. Spiriti [r], S. Squarcia [w], H. Staeck [v], C. Stanescu [r], G. Stavropoulos [z], F. Stichelbaut [ab], A. Stocchi [n], J. Strauss [b], R. Strub [aa], M. Szczekowski [ao], M. Szeptycka [ao], P. Szymanski [ao], T. Tabarelli [t], S. Tavernier [ab], G.E. Theodosiou [z], A. Tilquin [as], J. Timmermans [o], V.G. Timofeev [f], L.G. Tkatchev [f], T. Todorov [f], D.Z. Toet [o], O. Toker [ah], E. Torassa [ac], L. Tortora [r], M.T. Trainor [s], D. Treille [i], U. Trevisan [w], W. Trischuk [i], G. Tristram [x], C. Troncon [t], A. Tsirou [i], E.N. Tsyganov [f], M. Turala [aq], R. Turchetta [aa], M.-L. Turluer [c], T. Tuuva [ah], I.A. Tyapkin [f], M. Tyndel [d], S. Tzamarias [i], S. Ueberschaer [v], O. Ullaland [i], V. Uvarov [y], G. Valenti [ak], E. Vallazza [ac], J.A. Valls Ferrer [g], C. Vander Velde [ab], G.W. Van Apeldoorn [o], P. Van Dam [o], W.K. Van Doninck [ab], J. Varela [a], P. Vaz [i], G. Vegni [t], L. Ventura [ag], W. Venus [d], F. Verbeure [ab], L.S. Vertogradov [f], D. Vilanova [c], L. Vitale [q], E. Vlasov [y], S. Vlassopoulos [ap], A.S. Vodopyanov [f], M. Vollmer [v], S. Volponi [ak], G. Voulgaris [j], M. Voutilainen [ah], V. Vrba [r], H. Wahlen [v], C. Walck [m], F. Waldner [q], M. Wayne [aℓ], A. Wehr [v], M. Weierstall [v], P. Weilhammer [i], J. Werner [v], A.M. Wetherell [i], J.H. Wickens [ab], J. Wikne [ai], G.R. Wilkinson [s], W.S.C. Williams [s], M. Winter [aa], D. Wormald [ai], G. Wormser [n], K. Woschnagg [af], N. Yamdagni [m], P. Yepes [i], A. Zaitsev [y], A. Zalewska [aq], P. Zalewski [n], D. Zavrtanik [i],

E. Zevgolatakos [z], G. Zhang [v], N.I. Zimin [f], M. Zito [c], R. Zitoun [u], R. Zukanovich Funchal [x], G. Zumerle [ag] and J. Zuniga [g]

[a] *LIP, Av. Elias Garcia 14 - 1e, P-1000 Lisbon Codex, Portugal*
[b] *Institut für Hochenergiephysik, Österreichische Akademie der Wissenschaften, Nikolsdorfergasse 18, A-1050 Vienna, Austria*
[c] *DPhPE, CEN–Saclay, F-91191 Gif-Sur-Yvette Cedex, France*
[d] *Rutherford Appleton Laboratory, Chilton, Didcot OX11 0QX, UK*
[e] *Department of Physics, University of Lund, Sölvegatan 14, S-223 63 Lund, Sweden*
[f] *Joint Institute for Nuclear Research, Dubna, Head Post Office, P.O. Box 79, SU-101 000 Moscow, USSR*
[g] *Instituto de Fisica Corpuscular (IFIC), Centro Mixto Universidad de Valencia–CSIC, and Departamento de Fisica Atomica Molecular y Nuclear, Universidad de Valencia, Avda. Dr. Moliner 50, E-46100 Burjassot (Valencia), Spain*
[h] *Department of Physics, University of Bergen, Allégaten 55, N-5007 Bergen, Norway*
[i] *CERN, CH-1211 Geneva 23, Switzerland*
[j] *Physics Laboratory, University of Athens, Solonos Street 104, GR-10680 Athens, Greece*
[k] *Université Claude Bernard de Lyon, 43 Boulevard du 11 Novembre 1918, F-69622 Villeurbanne Cedex, France*
[l] *Institut für Experimentelle Kernphysik, Universität Karlsruhe, Pf. 6980, W-7500 Karlsruhe 1, FRG*
[m] *Institute of Physics, University of Stockholm, Vanadisvägen 9, S-113 46 Stockholm, Sweden*
[n] *Laboratoire de l'Accélérateur Linéaire, Université de Paris-Sud, Bâtiment 200, F-91405 Orsay, France*
[o] *NIKHEF-H, Postbus 41882, NL-1009 DB Amsterdam, The Netherlands*
[p] *Institut des Sciences Nucléaires, Université de Grenoble 1, F-38026 Grenoble, France*
[q] *Dipartimento di Fisica, Università di Trieste and INFN, Via A. Valerio 2, I-34127 Trieste, Italy and Istituto di Fisica, Università di Udine, Via Larga 36, I-33100 Udine, Italy*
[r] *Istituto Superiore di Sanità, Istituto Nazionale di Fisica Nucleare (INFN), Viale Regina Elena 299, I-00161 Rome, Italy*
[s] *Nuclear Physics Laboratory, University of Oxford, Keble Road, Oxford OX1 3RH, UK*
[t] *Dipartimento di Fisica, Università di Milano and INFN, Via Celoria 16, I-20133 Milan, Italy*
[u] *LPNHE, Universités Paris VI et VII, Tour 33 (RdC), 4 place Jussieu, F-75230 Paris Cedex 05, France*
[v] *Fachbereich Physik, Universität Wuppertal, Pf. 100 127, W-5600 Wuppertal 1, FRG*
[w] *Dipartimento di Fisica, Università di Genova and INFN, Via Dodecaneso 33, I-16146 Genoa, Italy*
[x] *Laboratoire de Physique Corpusculaire, Collège de France, 11 place M. Berthelot, F-75231 Paris Cedex 5, France*
[y] *Institute for High Energy Physics, Serpukhov, P.O. Box 35, SU-142 284 Protvino (Moscow Region), USSR*
[z] *Institute of Nuclear Physics, N.C.S.R. Demokritos, P.O. Box 60228, GR-15310 Aghia Paraskevi, Greece*
[aa] *Division des Hautes Energies, CRN–Groupe DELPHI and LEPSI, B.P. 20 CRO, F-67037 Strasbourg Cedex, France*
[ab] *Physics Department, Universitaire Instelling Antwerpen, Universiteitsplein 1, B-2610 Wilrijk, Belgium and IIHE, ULB–VUB, Pleinlaan 2, B-1050 Brussels, Belgium and Service de Physique des Particules Elémentaires, Faculté des Sciences, Université de l'Etat Mons, Av. Maistriau 19, B-7000 Mons, Belgium*
[ac] *Dipartimento di Fisica Sperimentale, Università di Torino and INFN, Via P. Giuria 1, I-10125 Turin, Italy*
[ad] *Dipartimento di Fisica, Università di Roma II and INFN, Tor Vergata, I-00173 Rome, Italy*
[ae] *Department of Physics, University of Liverpool, P.O. Box 147, Liverpool L69 3BX, UK*
[af] *Department of Radiation Sciences, University of Uppsala, P.O. Box 535, S-751 21 Uppsala, Sweden*
[ag] *Dipartimento di Fisica, Università di Padova and INFN, Via Marzolo 8, I-35131 Padua, Italy*
[ah] *Department of High Energy Physics, University of Helsinki, Siltavuorenpenger 20 C, SF-00170 Helsinki 17, Finland*
[ai] *Physics Department, University of Oslo, Blindern, N-1000 Oslo 3, Norway*
[aj] *Facultad de Ciencias, Universidad de Santander, av. de los Castros, E-39005 Santander, Spain*
[ak] *Dipartimento di Fisica, Università di Bologna and INFN, Via Irnerio 46, I-40126 Bologna, Italy*
[al] *Ames Laboratory and Department of Physics, Iowa State University, Ames, IA 50011, USA*
[am] *Universidad Complutense, Avda. Complutense s/n, E-28040 Madrid, Spain*
[an] *Niels Bohr Institute, Blegdamsvej 17, DK-2100 Copenhagen Ø, Denmark*
[ao] *Institute for Nuclear Studies, and University of Warsaw, Ul. Hoża 69, PL-00681 Warsaw, Poland*
[ap] *Physics Department, National Technical University, Zografou Campus, GR-15773 Athens, Greece*
[aq] *High Energy Physics Laboratory, Institute of Nuclear Physics, Ul. Kawiory 26 a, PL-30055 Cracow 30, Poland*
[ar] *School of Physics and Materials, University of Lancaster, Lancaster LA1 4YB, UK*
[as] *Université d'Aix - Marseille II, Case 907, 70, route Léon Lachamp, F-13288 Marseille Cedex 09, France*

Received 4 December 1991

The weak mixing angle has been measured from the charge asymmetry of hadronic events with two different approaches using the DELPHI detector at LEP. Both methods are based on a momentum-weighted charge sum to determine the jet charge in both event hemispheres. In a data sample of 247 300 multihadronic $Z^0$ decays a charge asymmetry of $\langle Q_F\rangle - \langle Q_B\rangle = -0.0076 \pm 0.0012(\text{stat.}) \pm 0.0005(\text{exp. syst.}) \pm 0.0014(\text{frag.})$ and a raw forward–backward asymmetry of $A_{FB}^{raw} = -0.0109 \pm 0.0020(\text{stat.}) \pm 0.0010(\text{exp. syst.}) \pm 0.0017(\text{frag.})$ have been measured. This result corresponds to a value of $\sin^2\theta_{eff} = 0.2345 \pm 0.0030(\text{exp.}) \pm 0.0027(\text{frag.})$, $\sin^2\theta_{\overline{MS}} = 0.2341 \pm 0.0030(\text{exp.}) \pm 0.0027(\text{frag.})$ and to $\sin^2\theta_w = 1 - m_W^2/m_Z^2 = 0.2299 \pm 0.0030(\text{exp.}) \pm 0.0027(\text{frag.}) \pm 0.0028(\text{theor.})$. The experimental error is the quadratic sum of the statistical and the experimental systematic error and the theoretical error originates from a value of $m_t = 130 \pm 40$ GeV/$c^2$ and a range of $m_H$ from 45 GeV/$c^2$ to 1000 GeV/$c^2$.

## 1. Introduction

The standard model of electroweak interactions predicts a forward–backward asymmetry in $e^+e^-$ collisions near the $Z^0$ peak which depends on the weak vector and axial-vector couplings of the $Z^0$ boson to fermion–antifermion pairs.

The differential $e^+e^-$ cross-section into a fermion pair $f\bar{f}$, where f means μ, τ, u, d, c, s, b can be expressed in the Born approximation as

$$\frac{d\sigma_f}{d\cos\theta} = \sigma_f^{TOT}(s)\left[\tfrac{3}{8}(1+\cos^2\theta) + A_{FB}^f(s)\cos\theta\right], \quad (1)$$

where $\theta$ is the production angle of the fermion f with respect to the incident electron line of flight and the forward–backward asymmetry is defined as

$$A_{FB}^f(s) = \frac{\sigma_F^f - \sigma_B^f}{\sigma_F^f + \sigma_B^f}, \quad (2)$$

where $\sigma_F^f$ and $\sigma_B^f$ are the fermion cross-sections in the forward and backward hemispheres, respectively. At the $Z^0$ resonance the forward–backward asymmetry is a direct measurement of parity-violating couplings. At tree level, apart from the photon channel terms suppressed by $(\Gamma_Z/M_Z)^2$, $A_{FB}$ is given by

$$A_{FB}^f(M_Z^2) \approx \frac{3}{4}\left(\frac{g_L^2 - g_R^2}{g_L^2 + g_R^2}\right)^e \left(\frac{g_L^2 - g_R^2}{g_L^2 + g_R^2}\right)^f \quad (3)$$

$$= \frac{3}{4}\frac{2v_e a_e}{v_e^2 + a_e^2}\frac{2v_f a_f}{v_f^2 + a_f^2}. \quad (4)$$

$g_L$ and $g_R$ are the left- and right-handed couplings of the fermions to the $Z^0$ and $v_f$ and $a_f$ are the vector and axial-vector couplings of the fermions,

$$v_f = I_3^f - 2Q_f \sin^2\theta_w, \quad a_f = I_3^f, \quad (5)$$

where $Q_f$ and $I_3^f$ denote the charge and weak isospin of the fermions. The indices e and f refer to the initial electron and final fermion, respectively. The u and d quark coupling constants have been measured in neutrino–nucleon scattering experiments [1].

Asymmetry measurements have been reported by LEP experiments for the leptonic decays of the $Z^0$, which yielded new determinations of the electroweak mixing angle $\sin^2\theta_w$ [2]. Measuring this asymmetry in the quark final states is also a crucial test of the theory, but is experimentally more difficult, since selecting pure samples of a given flavour requires specific tagging methods, which usually suffer from low efficiency. The currently available measurements, performed for c and b quarks, are still restricted by the limited statistics [3].

On the other hand the small remaining charge asymmetry averaged over all quark flavours,

$$A_{FB} = \frac{1}{\Gamma_{had}} \times (\Gamma_u A_{FB}^u - \Gamma_d A_{FB}^d + \Gamma_c A_{FB}^c - \Gamma_s A_{FB}^s - \Gamma_b A_{FB}^b), \quad (6)$$

can be measured without flavour tagging. The different signs in this sum for $+\frac{2}{3}$ and $-\frac{1}{3}$ charged quarks appear because experimentally only the charge in the two hemispheres is measured and not the flavour of the quarks so that u and c quarks enter with a positive sign while d, s and b quarks get negative signs. $\Gamma_f$ is the $Z^0$ partial decay width into quark f,

$$\Gamma_f = \frac{G_\mu m_Z^3}{8\sqrt{2}\,\pi}(v_f^2 + a_f^2), \quad (7)$$

and $\Gamma_{had}$ is the total hadronic width. On resonance ($\sqrt{s}=M_Z$), neglecting mass effects, the charge asymmetry can thus be expressed as

$$A_{FB}=\frac{3G_\mu m_Z^3}{8\sqrt{2}\,\pi\Gamma_{had}}\frac{v_e a_e}{v_e^2+a_e^2}\,(2v_u a_u-3v_d a_d)\,, \qquad (8)$$

and is of the order $-5\%$. However, the charge of the initial quarks is not directly accessible and the charge of the final hadron jets has to be evaluated. Techniques for this have already been used at lower energies [4–8] and recently with LEP data [9].

## 2. Detector description

A detailed description of the DELPHI apparatus can be found in ref. [10]. Only tracking detectors for charged particles are relevant for the present analysis: the inner detector (ID), the time projection chamber (TPC), the outer detector (OD) and the forward chambers A and B (FCA, FCB).

The trigger for hadronic events was based on combinations of tracking detectors offering redundancy, scintillator hodoscopes and calorimeters. The trigger efficiency was found to be higher than 99.9% during most of the data taking period.

## 3. Selection of events

Only charged particles were used for this analysis and were retained if they satisfied the following selection criteria:
- momentum $p$ between 0.4 and 50 GeV/$c$;
- track length above 50 cm;
- projection of impact parameter below 5 cm in the plane transverse to the beam direction;
- distance to the measured vertex along the beam direction below 4 cm.

The cut values were chosen so as to allow a reliable measurement of the multiplicity and momentum of the selected charged particles.

Using these charged particles, the sphericity was computed and its axis was defined as the event axis. As shown in fig. 1 the sphericity axis was oriented in the same direction as the incoming electron beam, with a polar angle $\theta$. Each event was then divided into two hemispheres on both sides of the plane transverse to the sphericity axis and passing through the measured vertex. A charged track was assigned to the forward and backward hemisphere if the component of its momentum along the sphericity axis was respectively positive or negative.

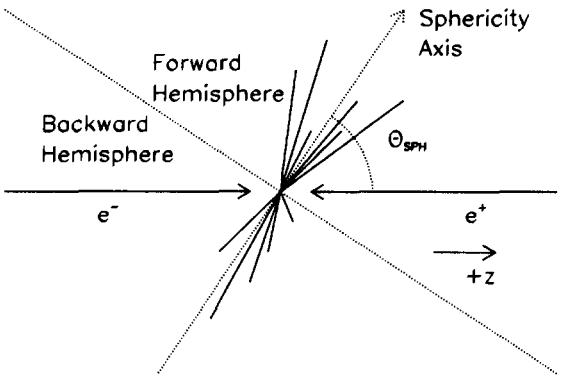


Fig. 1. Definition of the forward and backward hemispheres for hadrons.

Hadronic events were then accepted by requiring
- no charged track with momentum larger than 50 GeV/$c$;
- a charged multiplicity larger than or equal to 5:
- a total momentum $\Sigma|p|_i$ larger than 15 GeV/$c$;
- a total momentum larger than 3 GeV/$c$ in each hemisphere;
- a missing momentum $|\Sigma p_i|$ less than 30 GeV/$c$;
- a sphericity axis within $|\cos\theta|<0.9$.

These selections insured good agreement between data and Monte Carlo simulations. The selection efficiency was found to be around 75% without significant dependence on the quark flavour. A total of 247 300 hadronic events were retained from 1990 and 1991 data taking period.

## 4. Monte Carlo simulation

A detailed Monte Carlo simulation of the detector was necessary in order to check that the measured hadronic charge asymmetry was not biased by detector or reconstruction effects.

Higher order QED radiative corrections were taken into account by using the electron and positron structure functions from the DYMU3 program [11]. The fragmentation of the final states was based on the

JETSET 7.2 parton shower Monte Carlo [12] using the parameters as given in ref. [13].

The simulation of the detector included secondary interactions, the collection of electronic signals and their digitization. The total number of generated $q\bar{q}$ events was 150 000. The same analysis was applied to both the simulated and the real events.

## 5. Methods

The basic idea of measuring quark-asymmetries by a momentum-weighted charge sum is to make use of the statistical correlation between quark charge and jet charge. In each hemisphere defined by the unit sphericity vector $\boldsymbol{e}_S$ the jet charge was obtained from

$$Q_{F(B)} = \frac{\sum_i q_i p_i^\kappa}{\sum_i p^\kappa}, \quad \boldsymbol{p}_i \cdot \boldsymbol{e}_S > 0 \ (\boldsymbol{p}_i \cdot \boldsymbol{e}_S < 0) \,. \tag{9}$$

The sum runs over all selected charged particles, with measured electric charge $q_i$ and momentum $p_i$, inside this hemisphere (fig. 1). The exponent $\kappa$ is varied to give the particles optimal weights in the sum in order to take advantage from the leading particle effect; which is that the most energetic hadron is most probably formed from the original quark. The total error of $\sin^2\theta_w$ was found to be minimal for a value of $\kappa$ around 1 as will be discussed later. From the jet charges the charge flow $Q_{FB}$ and the total charge $Q_{TOT}$ were obtained:

$$Q_{FB} = Q_F - Q_B, \quad Q_{TOT} = Q_F + Q_B \,. \tag{10}$$

These two distributions are well described by the Monte Carlo simulation as shown in fig. 2.

In order to extract $\sin^2\theta_w$ from these observables two different methods were used. The first one is based on the fact that the mean value of the charge flow for each flavour depends upon $A_{FB}^f(\sin^2\theta_w)$. Denoting the number of events with a quark f produced in the forward hemisphere by $N_F^f$ with a charge flow $\langle Q_{FB}^{f,F} \rangle$ and the number of complementary events by $N_B^f$ with a charge flow $\langle Q_{FB}^{f,B} \rangle$, the mean charge flow

$$\langle Q_{FB}^f \rangle = \frac{N_F^f \langle Q_{FB}^{f,F} \rangle + N_B^f \langle Q_{FB}^{f,B} \rangle}{N_F^f + N_B^f} \tag{11}$$

is the weighted sum of both categories. The charge separation $\delta^f$

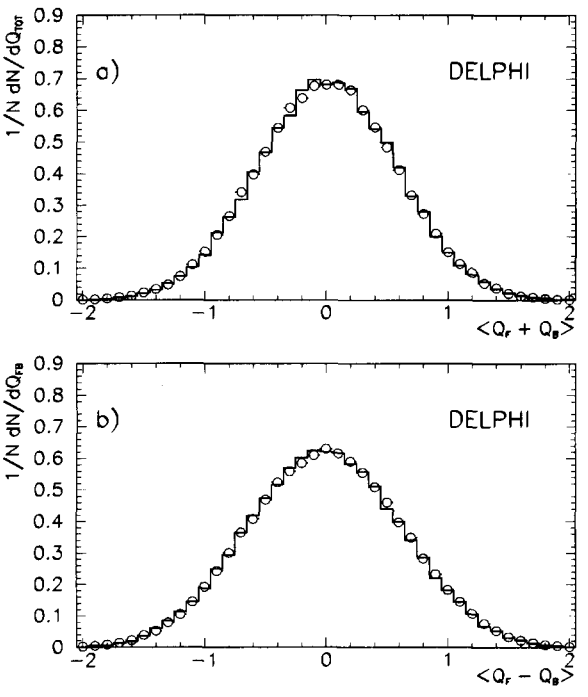


Fig. 2. Distributions (a) of the total charge $Q_{TOT}$ and (b) of the charge flow $Q_{FB}$: comparison between data points (circles) and Monte Carlo simulation (full line) for an exponent $\kappa = 1.0$.

$$\delta_F^f \equiv \langle Q_{FB}^{f,F} \rangle, \quad \delta_B^f \equiv \langle Q_{FB}^{f,B} \rangle \tag{12}$$

is at parton level $\delta^f = 2Q_f$ with $Q_f$ being the quark charge while at hadron level $\delta^f < 2Q_f$ (fig. 3). The only reason to expect a difference between $\delta_F^f$ and $-\delta_B^f$ are asymmetries in the detector. All effects that are included in the full detector Monte Carlo simulation lead to charge separations [#1] in forward and backward hemisphere that agree within the statistical error (table 1). Therefore in the following $\delta_F^f = -\delta_B^f$ is used, leading to

$$\langle Q_{FB}^f \rangle = \delta^f A_{FB}^f \,. \tag{13}$$

Experimentally only an averaged charge asymmetry is measured. This is the sum over the different flavours weighted by the relative production rates

$$\langle Q_{FB} \rangle = C_{acc} \sum_{f=1}^{5} \delta^f A_{FB}^f \frac{\Gamma_f}{\Gamma_{had}}, \tag{14}$$

[#1] One would expect naively $\delta^u = \delta^c$, $\delta^d = \delta^s = \delta^b$ and $\delta^u/\delta^d = \pm\frac{2}{3}/-\frac{1}{3} = -2$. But due to the difference in the fragmentation and decay of the various flavoured hadrons this is not fulfilled.

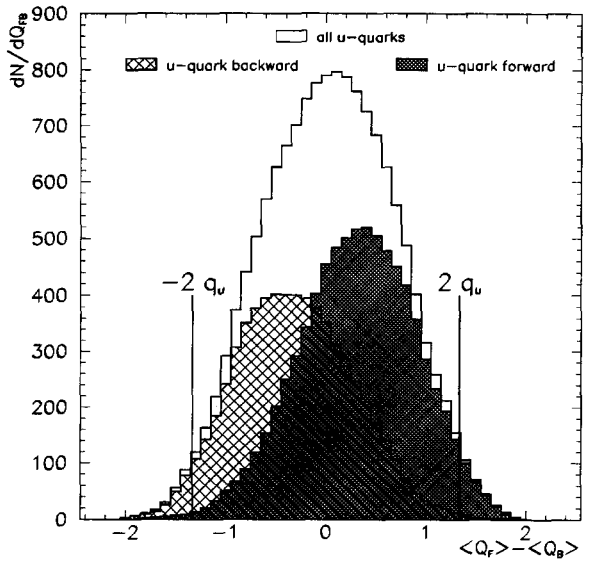


Fig. 3. Charge flow $Q_{FB}$ and charge separations $\delta_F^f$ and $\delta_B^f$ for u quarks after the full detector Monte Carlo simulation for $\kappa=1$.

Table 1
The charge separation $\delta_F^f$, $\delta_B^f$ and the efficiencies $\varepsilon_F^f$, $\varepsilon_B^f$ from the full detector Monte Carlo simulation using $\kappa=1$. The statistical errors are $\pm 0.01$.

| Flavour | $\delta_F^f$ | $\delta_B^f$ | $\varepsilon_F^f$ | $\varepsilon_B^f$ |
|---|---|---|---|---|
| d | −0.19 | +0.21 | 0.63 | 0.63 |
| u | +0.32 | −0.30 | 0.72 | 0.71 |
| s | −0.28 | +0.24 | 0.69 | 0.66 |
| c | +0.15 | −0.13 | 0.61 | 0.59 |
| b | −0.25 | +0.24 | 0.67 | 0.66 |

with the theoretical acceptance

$$C_{acc}=\frac{4\cos\theta_{max}}{3+\cos^2\theta_{max}} \tag{15}$$

which is in this analysis $C_{acc}=95\%$ for $\cos\theta_{max}=0.9$. Inserting eqs. (4) and (7) this can be written near the $Z^0$ resonance as

$$\langle Q_{FB}\rangle = C_{acc}\frac{3G_\mu m_Z^3}{8\sqrt{2}\,\pi\Gamma_{had}}\frac{v_e a_e}{v_e^2+a_e^2}\sum_{f=1}^{5}\delta^f v_f a_f . \tag{16}$$

The measured charge asymmetry $\langle Q_{FB}\rangle$ is translated into $\sin^2\theta_w$ by solving eq. (16). The basic principle of the method is similar to an analysis presented recently by the ALEPH collaboration [9].

In a second approach the flight direction of the positive quark is estimated on an event by event basis. This is done by using the *sign* of the charge flow in the event from which a raw forward–backward asymmetry $A_{FB}^{raw}$ is calculated:

$$A_{FB}^{raw}(f)=\frac{N_F^f-N_B^f}{N_F^f+N_B^F}, \tag{17}$$

$N_{F(B)}$ being the number of events with $Q_{FB}>0$ ($<0$). $A_{FB}^{raw}$ is related to $A_{FB}^f$ by

$$A_{FB}^{raw}(f)=C_{acc}(2\varepsilon^f-1)A_{FB}^f . \tag{18}$$

In this method the theoretical acceptance $C_{acc}$ is the same as above (eq. (15)). The efficiency $\epsilon^f$ of tagging the correct positive quark hemisphere, using $Q_{FB}$,

$$\varepsilon^f=\int_0^2 dQ_{FB}^{f,F}\Big/\int_{-2}^{2} dQ_{FB}^{f,F} \tag{19}$$

is taken from the Monte Carlo simulation and is given for the different flavours in forward and backward hemisphere in the second part of table 1. As for the $\delta^f$ the efficiencies in the two hemispheres agree within the statistical error and in the following $\varepsilon_F^f=\varepsilon_B^f$ is used.

Analogously to eq. (16) the value obtained for $A_{FB}^{raw}$ is related to the coupling constants $v_f$ and $a_f$ by

$$A_{FB}^{raw}=C_{acc}\frac{3G_\mu m_Z^3}{8\sqrt{2}\,\pi\Gamma_{had}}\frac{v_e a_e}{v_e^2+a_e^2}\sum_{f=1}^{5}(2\varepsilon_f-1)v_f a_f . \tag{20}$$

Neither method can directly determine $A_{FB}$ since the $\delta^f$ and $\varepsilon^f$ are different for the various quark flavours.

## 6. Experimental results

Table 2 shows the charge asymmetry and the raw forward–backward asymmetry values obtained by the above methods for different choices of the weighting parameter $\kappa$. These results are averaged over a range in centre of mass energy between 89 and 94 GeV. This is allowed since $\langle Q_{FB}\rangle$ varies almost linearly with the energy near the $Z^0$ resonance, so the average value will yield $\langle Q_{FB}\rangle$ at the $Z^0$ resonance if the number of

Table 2
Experimental results for the charge asymmetry ($\langle Q_{FB} \rangle$), for the raw forward–backward asymmetry ($A_{FB}^{raw}$) and the obtained values of $\sin^2\theta_{eff}$.

| $\kappa$ | $\langle Q_{FB} \rangle$ | $\sin^2\theta_{eff}$ | $A_{FB}^{raw}$ | $\sin^2\theta_{eff}$ |
|---|---|---|---|---|
| 0.5 | $-0.0051 \pm 0.0009$ | $0.2332 \pm 0.0034$ | $-0.0105 \pm 0.0020$ | $0.2351 \pm 0.0032$ |
| 1.0 | $-0.0076 \pm 0.0012$ | $0.2340 \pm 0.0029$ | $-0.0109 \pm 0.0020$ | $0.2351 \pm 0.0030$ |
| 1.5 | $-0.0096 \pm 0.0016$ | $0.2340 \pm 0.0028$ | $-0.0099 \pm 0.0020$ | $0.2362 \pm 0.0029$ |

events on the two sides of the resonance are similar, which is true in our case.

The calculation of $A_{FB}^{f}$ from $\sin^2\theta_w$ follows the formulae given by Djouadi et al. [14], where $\sin^2\theta_{eff}$ is defined as

$$\sin^2\theta_{eff} = \sin^2\theta_w + \frac{3\sqrt{2}\, G_\mu m_t^2}{16\pi^2} \cos^2\theta_w + \frac{\alpha}{4\pi}\left[\ln\left(\frac{m_H}{17.3\ \mathrm{GeV}/c^2} + 1\right) - 2\right] \quad (21)$$

with $\sin^2\theta_w = 1 - m_W^2/m_Z^2$. Additional electroweak corrections for the $Z^0$–$b\bar{b}$ vertex were applied [14]:

$$a_b \to a_b + \frac{2}{3}\frac{3\sqrt{2}\, G_\mu m_t^2}{16\pi^2},$$

$$v_b \to v_b + \frac{2}{3}\frac{3\sqrt{2}\, G_\mu m_t^2}{16\pi^2}. \quad (22)$$

Including QCD and QED corrections [14] in this improved Born approximation for $A_{FB}^{f}$ excellent agreement was found between the forward–backward asymmetry, as a function of $m_t$, obtained from the program ZFITTER [15] and the analytical calculations from ref. [14]. An additional correction was applied to the b quark asymmetry taking $B\bar{B}$ mixing into account using a full detector Monte Carlo simulation. A value of $\bar{\chi} = 0.132 \pm 0.026$ [16] reduces $\delta^b$ by $(21.8 \pm 5.3)\%$ and $\varepsilon^b$ by $(3.8 \pm 3.3)\%$.

The values for $\sin^2\theta_{eff}$ given in table 2 were obtained including all the corrections to the Born level mentioned above using the following parameters:

$$m_Z = 91.18\ \mathrm{GeV}/c^2, \quad m_t = 130\ \mathrm{GeV}/c^2,$$
$$m_H = 300\ \mathrm{GeV}/c^2,$$
$$\alpha(m_Z^2) = 1/127.6, \quad \alpha_s = 0.120,$$
$$G_\mu = 1.16637 \times 10^{-5}\ \mathrm{GeV}/c^2, \quad (23)$$

and the charge separations $\delta_F^f$ and the efficiencies $\varepsilon_F^f$ as given in table 1.

The weak dependence of $\sin^2\theta_{eff}$ on the choice of the weighting parameter $\kappa$ in table 2 will be included in the systematic error. Note that the statistical errors given in table 2 are nearly 100% correlated.

### 6.1. Experimental systematic error

The systematic error for detector imperfections influences both the measured values of $\langle Q_{FB} \rangle$ ($A_{FB}^{raw}$) and the efficiencies $\delta^f$ ($\varepsilon^f$) determined from the Monte Carlo simulation. To give a consistent picture a systematic error on $\langle Q_{FB} \rangle$ ($A_{FB}^{raw}$) is calculated from the observed variation of $\sin^2\theta_{eff}$.

Both methods rely on the fact that the Monte Carlo simulation describes the charge flow correctly. For gaussian distributions like $Q_{FB}$ and $Q_{TOT}$ (fig. 2) the width and the mean value are statistically independent. The measurement of the widths, which is independent of $A_{FB}$, is therefore a good test for the Monte Carlo simulation. In fig. 4 the good agreement between experimental data and Monte Carlo simulation is shown for $\sigma_{Q_{FB}}$ and $\sigma_{Q_{TOT}}$ together with the values obtained for $\langle Q_{TOT} \rangle$ for different choices of the weighting parameter $\kappa$.

The deviation from zero of $\langle Q_{TOT} \rangle$ in data and Monte Carlo can be understood from secondary interactions in the detector. The larger nuclear cross-section for $\pi^-$p scattering than for $\pi^+$p scattering at small $Q^2$ leads to an excess of low momenta positive tracks. With the increase of the weighting parameter $\kappa$ the high momentum particles get more and more weight in the calculation of the jet charges $Q_F$ and $Q_B$ and the observed values for $\langle Q_{TOT} \rangle$ get closer to 0. If these interactions are as well asymmetric in the two $z$-hemispheres, they lead to systematic errors in the measurement of $\sin^2\theta_{eff}$. To study this a momentum cut of $p \geq 2.5\ \mathrm{GeV}/c$ was applied since most particles

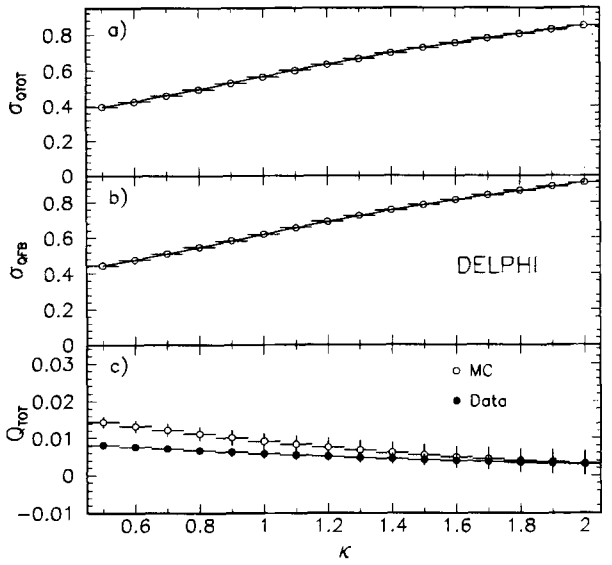


Fig. 4. Comparison between data points (circles) and Monte Carlo simulation (full line) for (a) the width of the total charge, (b) the width of the charge flow and (c) the mean value of the total charge, for different exponents $\kappa$.

from these processes are slow (table 3). Furthermore the complete analysis was repeated using only positive (negative) tracks and the observed variation of $\sin^2\theta_{\text{eff}}$ was included in the systematic error (table 3).

Other sources of systematic uncertainties are the assignment of unphysically high momenta to charged particles, mainly as a result of reconstruction ambiguities due to overlapping tracks. These effects were studied by using only particles with momentum below 25 GeV/$c$ (table 3).

The choice of the weighting parameter $\kappa$ should have no influence on the obtained value for $\sin^2\theta_{\text{eff}}$. For both methods the statistical and systematical error were found to be minimal for $\kappa$ around 1. The variation of $\sin^2\theta_{\text{eff}}$ with $\kappa$ between 0.5 and 1.5 is given in table 3. $\sin^2\theta_{\text{eff}}$ was found to be stable for $\kappa$ greater than 1.5.

Finally the limited Monte Carlo statistics leads to a systematic error on $\sin^2\theta_{\text{eff}}$ of 0.3% which corresponds to an systematic error on $\langle Q_{\text{FB}}\rangle$ of 3% and on $A_{\text{FB}}^{\text{raw}}$ of 3.6%.

The total systematic error is determined to be $^{+6.9}_{-4.9}$% on the charge asymmetry and $^{+6.5}_{-12.2}$% on the raw forward–backward asymmetry. Since all the systematic uncertainties given in table 3 are small compared to the statistical error it is not useful to give an asymmetric error at that level of accuracy. Therefore the total systematic error from the experiment is estimated to be $\pm 6$% on the charge asymmetry and $\pm 9$% on the raw forward–backward asymmetry.

### 6.2. Systematic error: fragmentation

The determination of the fermion charge has other systematic uncertainties in addition to those arising from the detector. Since after hadronisation the quark charge is no longer directly accessible, it is statistically reconstructed from the momentum-weighted charged hadron spectrum. This spectrum is modelled by string fragmentation and depends on the choice of the parameters in the Monte Carlo simulation.

The impact on the charge asymmetry $\langle Q_{\text{FB}}\rangle$ and the raw asymmetry $A_{\text{FB}}^{\text{raw}}$ from the variation of different parameters in the JETSET 7.2 parton shower Monte Carlo has been studied as can be seen from table 4. For the parameters which lead to the largest contribution to the systematic error on $\langle Q_{\text{FB}}\rangle$ and $A_{\text{FB}}^{\text{raw}}$ the variations in the charge separation $\delta^{\text{f}}$ and

Table 3
Systematic error of $\langle Q_{\text{FB}}\rangle$ and $A_{\text{FB}}^{\text{raw}}$ from the experiment.

| Method to obtain systematic uncertainty | Charge asymmetry $\Delta\langle Q_{\text{FB}}\rangle/\langle Q_{\text{FB}}\rangle$ (%) | Raw asymmetry $\Delta A_{\text{FB}}^{\text{raw}}/A_{\text{FB}}^{\text{raw}}$ (%) |
|---|---|---|
| cut: $p \geq 2.5$ GeV/$c$ | +3.7 | −3.6 |
| cut: $p_{\max} \leq 25$ GeV/$c$ | −3.7 | −3.6 |
| using only positive or negative tracks | +4.9 | −9.0 |
| variation of $\kappa$ (0.5–1.5) | ±1.0 | ±5.4 |
| limited Monte Carlo statistics | ±3.0 | ±3.6 |
| total systematic error | $^{+6.9}_{-4.9}$ | $^{+6.5}_{-12.2}$ |

Table 4
Relative systematic error of the charge asymmetry $\langle Q_{FB} \rangle$ and of the raw asymmetry $A_{FB}^{raw}$ calculated from the $\delta^f$ respectively $\varepsilon^f$ resulting from different Monte Carlo parameter sets.

| Parameter | Range | $\Delta\langle Q_{FB}\rangle/\langle Q_{FB}\rangle$ (%) | $\Delta A_{FB}^{raw}/A_{FB}^{raw}$ (%) |
|---|---|---|---|
| s/u | 0.27–0.36 | 5.3 | 4.2 |
| $\delta_{P_T}$ | 340–410 | 1.0 | 1.5 |
| Lund $A$ | 0.125–0.325 | 2.8 | 0.3 |
| Lund $B$ | 0.2–0.4 | 1.6 | 1.8 |
| $\epsilon_b$ | $(3\text{–}10)\times10^{-3}$ | 2.2 | 1.7 |
| $\epsilon_c$ | $(2\text{–}71)\times10^{-3}$ | 3.7 | 2.1 |
| $\Lambda_{QCD}$ | 260–400 | 3.3 | 1.6 |
| [V/(V+PS)](u, d) | 0.34–0.54 | 1.1 | 1.3 |
| [V/(V+PS)](s) | 0.5–0.75 | 2.0 | 2.1 |
| [V/(V+PS)](c, b) | 0.66–0.8 | 2.4 | 3.0 |
| $M_{Stop}$ | 1.0–2.0 | 0.3 | 0.6 |
| $\bar{\chi}$ | 0.11–0.16 | 4.2 | 7.5 |
| PS-ME string frag. | – | 6.2 | 5.2 |
| PS-ME ind. frag. | – | 13.6 | 10.0 |
| total error | | 18.0 | 15.2 |

the tagging efficiency $\varepsilon^f$ are given in table 5 for each flavour separately. The effect on $\langle Q_{FB} \rangle$ ($A_{FB}^{raw}$) was computed from eq. (16) ((20)) with an asymmetry taken from the Born approximation for $\sin^2\theta_w = 0.23$.

The DELPHI Monte Carlo using hybrid fragmentation differs slightly from the tuning in ref. [13]: Lund $A/B = 0.225/03$, $\epsilon_c/\epsilon_b = 0.025/0.005$, $\sigma_{P_T} = 410$ MeV. The variations in the given ranges are motivated by the following considerations:

- Ratio of s quarks tunnelling into the string to u quarks (s/u). Here a recent measurement of the TPC/2γ Collaboration [17] is referred to.
- $\sigma_{P_T}$: the interval covers the full range of measured values from various experiments [13,18,19].
- Parameters $A$ and $B$ of the Lund symmetric fragmentation function. These two parameters were varied in the ranges compatible with DELPHI data.
- Parameters $\epsilon_c$ and $\epsilon_b$ of the Peterson fragmentation function. In order to estimate this effect, the (rather large) range from ALEPH [9] is taken.
- $\Lambda_{QCD}$: the variation covers the region between the TASSO [13] and MARK II [18] tunings.
- Ratio of vector-mesons to all mesons [V/(V+PS)]: this has been varied around the defaults taking into account theoretical limits as well as the precision of a CELLO-measurement [20] for strange mesons. No large effect on rapidity fitting (although one might expect this since it affects multiplicity) was found.
- $M_{Stop}$: the lower limit of the gluon-branching cutoff in the parton cascade is taken to be safely away from the breakdown of perturbation theory due to small momentum transfer. The upper limit comes from comparison with DELPHI rapidity and aplanarity distributions.
- $B\bar{B}$-mixing: A range corresponding to the measured value of $\bar{\chi} = 0.132 \pm 0.026$ [16], a weighted mixture of the $B_d$ and $B_s$ mixing parameters, was used to obtain the variation of $\langle Q_{FB} \rangle$ ($A_{FB}^{raw}$).

In addition, Monte Carlo events from the second order matrix element calculation (JETSET 7.2 ME) using string-fragmentation and independent-fragmentation models based on the tuning in ref. [21] were studied and deviations from parton shower data are regarded as additional systematic errors. The result of this comparison can be found in the last two rows of table 4 indicated by "PS-ME string frag." and "PS–ME ind. frag." respectively.

The total systematic error from the fragmentation on $\langle Q_{FB} \rangle$ and $A_{FB}^{raw}$ is the quadratic sum of the contributions:

$$\frac{\Delta\langle Q_{FB}\rangle}{\langle Q_{FB}\rangle} = 18.0\%, \quad \frac{\Delta A_{FB}^{raw}}{A_{FB}^{raw}} = 15.2\%. \qquad (24)$$

Table 5
Relative systematic error of the charge separations $\delta^f$ and the tagging efficiency $\varepsilon^f$ specified for each flavour and total contribution to $\langle Q_{FB} \rangle$ and $A_{FB}^{raw}$.

| | Parameter | | | | |
|---|---|---|---|---|---|
| | s/u | $\epsilon_c$ | $\Lambda_{QCD}$ | PS-ME string frag. | PS-ME ind. frag. |
| Range | 0.27–0.36 | $(2\text{–}71)\times 10^{-3}$ | 260–400 | | |
| $\frac{\Delta\delta^d}{\delta^d}$ (%) | 3.0±0.8 | 1.0±0.7 | 3.7±1.1 | 4.2±0.7 | 7.4±0.7 |
| $\frac{\Delta\varepsilon^d}{\varepsilon^d}$ (%) | 2.0±1.5 | 1.0±1.7 | 1.2±1.7 | 4.5±1.4 | 2.4±1.4 |
| $\frac{\Delta\delta^u}{\delta^u}$ (%) | 1.1±0.5 | 0.7±0.5 | 3.1±0.8 | 5.3±0.4 | 16.1±0.6 |
| $\frac{\Delta\varepsilon^u}{\varepsilon^u}$ (%) | 1.1±1.3 | 0.5±1.3 | 0.5±1.2 | 5.9±1.0 | 21.1±1.3 |
| $\frac{\Delta\delta^s}{\delta^s}$ (%) | 2.3±0.6 | 0.9±0.6 | 6.0±0.9 | 4.1±0.5 | 4.6±0.6 |
| $\frac{\Delta\varepsilon^s}{\varepsilon^s}$ (%) | 1.3±1.4 | 0.8±1.2 | 1.6±1.4 | 3.4±1.2 | 1.4±1.2 |
| $\frac{\Delta\delta^c}{\delta^c}$ (%) | 4.2±1.2 | 16.8±1.2 | 2.7±1.6 | 4.8±0.9 | 31.7±1.5 |
| $\frac{\Delta\varepsilon^c}{\varepsilon^c}$ (%) | 4.0±2.1 | 9.7±2.1 | 0.8±2.9 | 4.1±2.4 | 35.9±3.0 |
| $\frac{\Delta\delta^b}{\delta^b}$ (%) | 2.2±0.6 | 0.8±0.7 | 0.8±0.7 | 2.9±0.4 | 0.4±0.5 |
| $\frac{\Delta\varepsilon^b}{\varepsilon^b}$ (%) | 2.2±1.3 | 0.9±1.1 | 0.8±1.2 | 2.6±1.0 | 1.0±1.1 |
| $\frac{\Delta\langle Q_{FB}\rangle}{\langle Q_{FB}\rangle}$ (%) | 5.3±0.7 | 3.7±0.7 | 3.3±1.0 | 6.2±0.6 | 13.6±0.5 |
| $\frac{\Delta A_{FB}^{raw}}{A_{FB}^{raw}}$ (%) | 4.2±1.6 | 2.1±1.6 | 1.5±1.5 | 5.2±1.2 | 10.0±1.1 |

## 7. Summary and conclusion

Using two different approaches to obtain $\sin^2\theta_{eff}$ a significant charge asymmetry of

$$\langle Q_{FB} \rangle - 0.0076 \pm 0.0012\,(\text{stat.}) \pm 0.0005\,(\text{exp. syst.}) \pm 0.0014\,(\text{frag.}) \quad (25)$$

and a raw forward–backward asymmetry of

$$A_{FB}^{raw} = -0.0109 \pm 0.0020\,(\text{stat.}) \pm 0.0010\,(\text{exp. syst.}) \pm 0.0017\,(\text{frag.}) \quad (26)$$

were found. From these two measurements $\sin^2\theta_{eff}$ was calculated to be $\sin^2\theta_{eff} = 0.2340 \pm 0.0029\,(\text{stat.}) \pm 0.0009\,(\text{exp. syst.}) \pm 0.0028\,(\text{frag.})$ from the charge asymmetry and $\sin^2\theta_{eff} = 0.2351 \pm 0.0030\,(\text{stat.}) \pm 0.0016\,(\text{exp. syst.}) \pm 0.0027\,(\text{frag.})$ from the raw forward–backward asymmetry, following the formulae given by Djouadi et al. [14]. Both results agree well within the experimental systematic error. The mean value of

$$\sin^2\theta_{eff} = 0.2345 \pm 0.0030\,(\text{exp.}) \pm 0.0027\,(\text{frag.}), \quad (27)$$

which is in the $\overline{\text{MS}}$ scheme

$$\sin^2\theta_{\overline{\mathrm{MS}}} = 0.2341 \pm 0.0030(\mathrm{exp.}) \pm 0.0027(\mathrm{frag.}), \quad (28)$$

corresponds to a value of $\sin^2\theta_w$, defined by $\sin^2\theta_w = 1 - m_W^2/m_Z^2$, of

$$\sin^2\theta_w = 0.2299 \pm 0.0030(\mathrm{exp.}) \pm 0.0027(\mathrm{frag.}) \pm 0.0028(\mathrm{theor.}), \quad (29)$$

using $m_t = 130$ GeV/$c^2$ and $m_H = 300$ GeV/$c^2$. The experimental error is the quadratic sum of the statistical and the experimental systematic error. The theoretical error originates from the uncertainty of $m_t = 130 \pm 40$ GeV/$c^2$ ($\Delta \sin^2\theta_w = \pm 0.0026$) and from the range of $m_H = 45$–$1000$ GeV/$c^2$ ($\Delta \sin^2\theta_w = \pm 0.0009$).

These results are in good agreement with a previous measurement [9]. The error is still dominated by the experimental statistics. Further data taking at LEP will therefore lead to a better measurement of $\sin^2\theta_{\mathrm{eff}}$ by the methods outlined in this letter.

## Acknowledgement

We are greatly indebted to our technical collaborators and to the funding agencies for their support in building and operating the DELPHI detector, and to the members of the CERN-SL Division for the excellent performance of the LEP collider.

## References

[1] U. Amaldi et al., Phys. Rev. D 36 (1987) 1385.
[2] F. Dydak, Results from LEP and the SLC, Proc. XXVth Intern. Conf. on High energy physics (Singapore, August 1990), eds. K.K. Phua and Y. Yamaguchi (1991) p. 3.
[3] ALEPH Collab., D. Decamp et al., Phys. Lett. B 263 (1991) 112;
L3 Collab., B. Adeva et al., Phys. Lett. B 252 (1990) 713.
[4] Amy Collab., D. Stuart et al., Phys. Rev. Lett. 64 (1990) 983.
[5] JADE Collab., T. Greenshaw et al., Z. Phys. C 42 (1989) 1.
[6] Mac Collab., W.W. Ash et al., Phys. Rev. Lett. 58 (1987) 1080.
[7] PLUTO Collab., Ch. Berger et al., Nucl. Phys. B 214 (1983) 189.
[8] TASSO Collab., R. Brandelik et al., Phys. Lett. B 100 (1981) 357.
[9] ALEPH Collab., D. Decamp et al., Phys. Lett. B 259 (1991) 377.
[10] DELPHI Collab., P. Aarnio et al., Nucl. Instrum. Methods A 303 (1991) 233.
[11] J.E. Campagne and R. Zitoun, Z. Phys. C 43 (1989) 469; in: Proc. Brighton Workshop on Radiative corrections (Sussex, July 1989).
[12] T. Sjostrand, Comput. Phys. Commun. 39 (1986) 347;
T. Sjostrand and M. Bengtsson, Comput. Phys. Commun. 43 (1987) 367, Version 7.2.
[13] TASSO Collab., W. Braunschweig et al., Z. Phys. C 41 (1988) 359.
[14] A. Djouadi, J.H. Kühn and P.M. Zerwas, Z. Phys. C 46 (1990) 411.
[15] D. Bardin et al., A users guide to ZFITTER: an analytical program for fermion pair production in $e^+e^-$ annihilation.
[16] ALEPH Collab., D. Decamp et al., Phys. Lett. B 244 (1990) 551.
[17] TPC/2γ Collab., M. Ronan, Talk XXVI Rencontres the Moriond on High energy in hadronic interactions (Les Arcs, Savoie, France, March 1991).
[18] MARK II Collab., A. Peterson et al., Phys. Rev. D 37 (1988) 1.
[19] Amy Collab., Y.K. Li et al., Phys. Rev. D 41 (1990) 2675.
[20] CELLO Collab., H.-J. Behrend et al., Z. Phys. C 46 (1990) 397.
[21] W. de Boer, H. Fürstenau and J.H. Köhne, Z. Phys. C 49 (1991) 141.